RESULTS AND PERFORMANCE SIMULATIONS OF THE MAIN LINAC DESIGN FOR B*ERL*inPro*

A. Neumann†, W. Anders, J. Knobloch, Helmholtz-Zentrum Berlin, Berlin, Germany

B. Riemann, T. Weis, TU Dortmund University, Dortmund, Germany

K. Brackebusch, T. Flisgen, T. Galek, K. Papke, U. van Rienen, Rostock University, Rostock, Germany

Abstract

The Berlin Energy Recovery Linac Project (B*ERL*inPro) is designed to develop and demonstrate CW LINAC technology for 100-mA-class ERLs. High-current operation requires an effective damping of higher order modes (HOMs) of the 1.3 GHz main linac cavities.

We have studied elliptical seven cell cavities damped by five waveguides at the adjacent beam tubes. Eigenmode calculations for geometrical figures of merit show that the present design should allow successful cw linac operation at the maximum beam current of 100 mA / 77pC bunch charge.

In this paper the progress in HOM calculations to avoid beam-breakup instabilities for the favored cavity structure is presented.

INTRODUCTION

B*ERL*inPro will be a CW driven ERL machine with a maximum current of 100 mA beam and a maximum energy of 50 MeV, while preserving a normalized emittance of better than 1 mm mrad at a pulse length of 2 ps [1]. The main linac cavity has strong HOM damping requirements since it is passed by two 100 mA beams that both resonantly interact with transverse deflecting (e.g. TM_{110}) cavity modes, leading to beam break up (BBU) [2].

An ERL cavity design must minimize the HOM's $R/Q_\perp$ and external quality factors Q_{ext} [8]. The mid-cell design influences the HOM spectrum, dispersion relation and operational mode acceleration performance (see [8] for op. mode parameters of the tuned structure). By proper end-cell tuning that preserves field flatness for the fundamental TM_{010}-π mode, mode localization (trapping) can be avoided and the Q_{ext} can be recuced to a sufficient extent.

In this paper updated HOM calculations of the main linac cavity using new methods are presented [8], and an outlook on ongoing activities to decompose the cavity structure into smaller parts is given [5] [9].

STRUCTURE EIGENMODE CALCULATIONS

The design under consideration is a seven cell structure using the Cornell ERL mid-cell design [6] and combining it
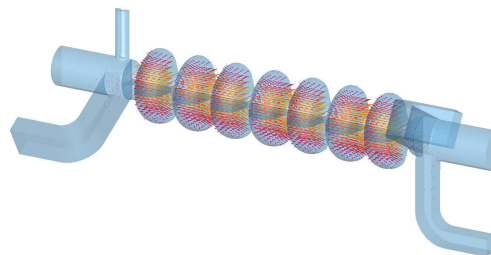
Figure 1: Rendering of the cavity design under consideration for B*ERL*inPro with a cut through the symmetry (FPC) plane and electric field magnitude of the operational mode.

Table 1: Cavity mid-cell figures of merit comparison.

	ERL shape Cornell U.	Spline shape TU Do, v4 / v5
E_{surf}/E_{acc} (π mode)	2.07	2.08 / 2.07
$R_\parallel/Q$ (π mode)	111 Ω	113 Ω / 112 Ω
intercell coupling κ	2.1 %	1.7 % / 1,9 %
Geometry factor G	272.7 Ω	- / 269.5 Ω

with JLab 3-fold symmetric waveguide HOM couplers [7] (see Figure 1). Flexible input power coupling is enabled by replacing one waveguide with a TTF-III type coaxial fundamental power coupler (thus breaking the 3-fold symmetry). The design aims at combing the peak field properties of the Cornell design with the advantage of waveguide couplers having a natural cutoff above the fundamental, and further limiting the possibility of dust intruding from ferrite beam tube absorbers into the cavity.

Base cells

In parallel to periodic boundary mid-cell calculations, such calculations were also performed using Spline-based cells [4]. Table 1 shows a preliminary comparison between 36 mm radius mid-cells for both designs. At the moment, development concentrates on the Cornell ERL mid-cell. Further development and degree elevation of the spline design may lead to a mid-cell shape with higher performance.

Transverse shunt impedance

The final goal will be to minimize the product $R/Q_\perp \cdot Q_{ext}$ for all HOMs. $|\vec{V}_\perp|^2 \propto R_\perp/Q$ can be computed di-
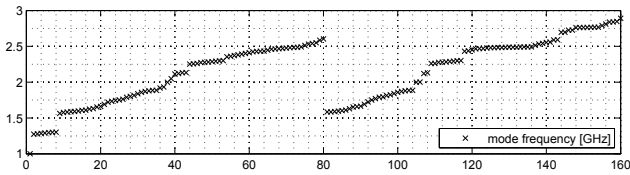
Figure 2: Frequency of all modes up to 2.85 GHz, about the lower range of the 4th dipole band. All modes were computed using the JDM eigenmode solver of CST MWS^{TM}.
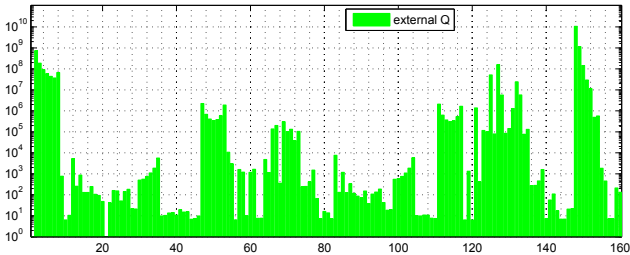

Figure 3: External Q of all TM/TE modes up to 2.85 GHz. While the dipole modes are sufficiently damped, some quadrupole modes exhibit large $Q_{ext} > 1 \cdot 10^6$.

rectly from the fields on the central axis by

$$\vec{V}_\perp = \frac{1}{q} \int \vec{F}_L(s) \exp\left(ik_\beta s\right) \, \mathrm{d}s \cdot \exp(-\mathrm{i}\Psi_0) \in \mathbb{R}^2 \quad (1)$$

simultaneously with its polarization and additional information about optimal phase relations in Ψ_0 [3]. The resulting $R/Q_\perp$ is shown in Figure 4. Again the dipole modes seem sufficiently damped while some quadrupole modes due to their high Q_{ext} and a small, but finite non-zero shunt impedance on axis show to be the most harming modes concerning BBU.
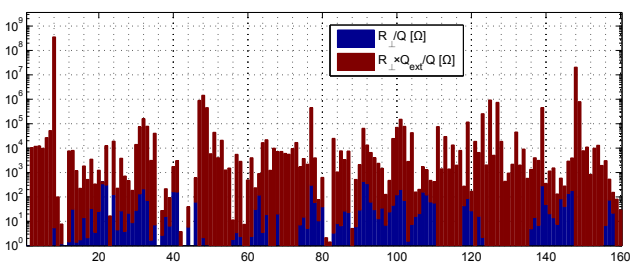

Figure 4: Transverse $R/Q_\perp$ and $R/Q_\perp \cdot Q_{ext}$ for all TM and TE modes up to 2.85 GHz (beginning of 4th dipole band). The arrow marks the coupler kick by the TTF-III power coupler at the fundamental mode.

Polar path analysis

The action of seemingly small voltages from mainly quadrupolar modes, giving rise to large instabilities, leads to the question if and to which extent quadrupole mode damping should be considered in realistic cavity designs, based on the influence of higher order mode coupler kicks

and imperfections in beam path position and construction issues. Due to the broken rotational symmetry, any eigenmode may consist of different multipole components. A scheme named polar path analysis was developed [3] to extract the voltage components a_p, b_p of the longitudinal (and equivalently, transverse) voltage

$$V_\parallel(r, \phi) \approx \sum_p r^p[b_p \cos(p\phi) + a_p \sin(p\phi)] \quad (2)$$

from all available longitudinal and transverse voltages on an arbitrary number of integration paths N (the different paths are comprised into vectors of the respective voltages) by constructing and pseudo-inverting a rectangular matrix $\mathbf{A}$ in an equation system of the form [3]

$$\begin{pmatrix} \vec{V}_\parallel \\ \omega\vec{V}_x \\ \omega\vec{V}_y \end{pmatrix} = \mathbf{A} \begin{pmatrix} \vec{a} \\ \vec{b} \end{pmatrix}. \quad (3)$$

To investigate the possible shift of quadrupole modes a calculation of $R_\perp/Q$ along circular distributed integration paths at an arbitrary offset of 5mm was performed. Fig. 5 shows the results of the eigenmode computation for a mode with a dominating quadrupole component. Fig. 6 is a plot of the reconstructed transverse area with the result coefficients $|a_0 + \mathrm{i}b_0| = 3,5 \cdot 10^4$ V (monopole), $|a_1 + \mathrm{i}b_1| = 1.28 \cdot 10^5$ V/mm (dipole) $|a_3 + \mathrm{i}b_3| = 4.6 \cdot 10^4$ V/mm^2 (quadrupole) and $|a_4 + \mathrm{i}b_4| = 5.6 \cdot 10^2$ V/mm^3 (sextupole).

For quadrupolar modes, we are interested in the shift of the transverse forceless path. Fig. 6 also shows the marked forceless point given as a solution of the complex polynomial $X(z) \stackrel{!}{=} 0$ [3].
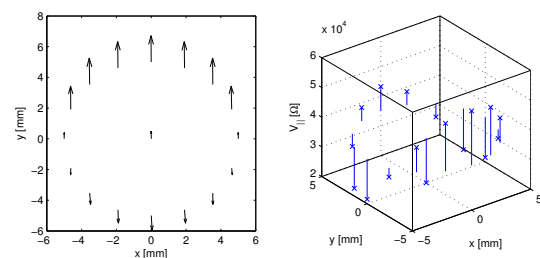

Figure 5: Polar plot of transverse (left, arrows) and longitudinal (right) voltages determined on circularly arranged integration paths at 5mm offset from beam axis for a mainly quadrupolar mode.

Most modes of these quadrupole bands are shifted more than the expected vertical beam size in the linac and thus mainly quadrupole modes may exhibit a non-neglectible dipole component. This effect needs to be investigated in more detail and it has to be understood how much the coupler's position influences this effective dipole component of the quadrupole modes.
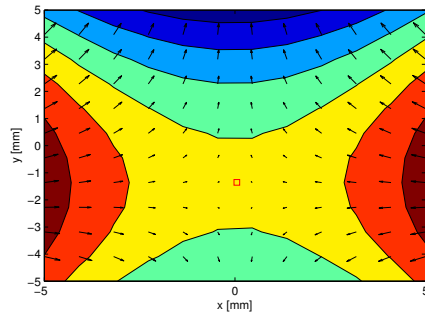
Figure 6: Reconstruction of the transverse (arrows) and longitudinal (isolines) voltages in the beam area from the data shown in Fig. 5. The red square marks the transverse forceless point.
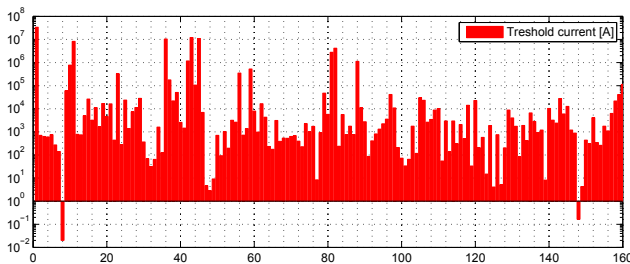

Figure 7: Approximate (orders of magnitude) calculations for the treshold current based on Eq. 4.

Treshold current

To evaluate and optimize the cavity, we use a simpflied equation for the treshold current

$$I_{\text{th}} \approx \frac{2c}{e} \frac{E_0}{R_\perp/Q \, Q_{\text{ext}} \omega} \quad (4)$$

for one cavity HOM that still depends on the mode's transverse shunt impedance $R/Q_\perp$, its external quality factor Q_{ext} and frequency ω and the beam's energy E_0, but neglects the influence of recirculation time and the recirculation arc linear beam optics ("worst phase" assumption).

The results of our preliminary treshold current calculation for all modes are shown in Fig. 7. The seemingly smallest current value is not valid due to being equivalent to a coupler kick of the operational mode which is externally driven and cannot be described by the treshold current formula.

OUTLOOK

Full 3d structure eigenmode computations using several million mesh cells for hundreds of modes need too much computational resources to implement them as iteration steps into an optimizer routine for end-cell tuning (to lower the Q_{ext} for the dangerous HOMs). Thus, the next steps in BERLinPro main linac cavity design will either consist of using Coupled S-parameter Calculations [11] of the seg-
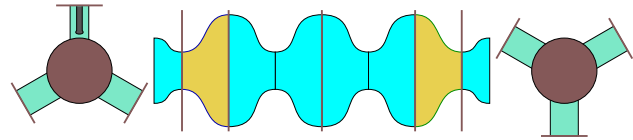

Figure 8: Cavity separation planned for CSC. The rotationally symmetric structure is decomposed along the equator radii, with an additional separation at the outer endcell iris. The resulting structure is concatenated with the 3d FPC/waveguide damping structure and the 2d (cartesian) 3-fold symmetric waveguide damping structure.

mented structure (see Fig. 8) with 2d eigenmode calculations of the rotationally symmetric cavity, or using a state-space equation system with a similarly separated structure [9] to find a set of end-cells with field-flat op. modes that are then optimized for maximum overall HOM damping $(R_\perp/Q \cdot Q_{\text{ext}})$ [5]. The sufficient cavity sets will then be concatenated to the full three cavity string, as already the lowest order dipole modes propagate along the beam tube and couple to the neighboring rf structures.

REFERENCES

[1] M. Abo-Bakr et al., "BERLinPro - A Compact Demonstrator ERL for High Current and Low Emittance Beams", LINAC'10, Tsukuba, September 2010,.

[2] Y. Petenev et al., "Modeling of the Beam Break Up Instability for BERLinPro ", IPAC'11, San-Sebstian, September 2011, MOPS051, p. 718, http://www.JACoW.org

[3] B. Riemann et al., "Alternative approaches for HOM-damped cavities," MOPB066, these proceedings

[4] B. Riemann et al., "Design of SRF cavities with profiles based on Bezier splines", ICAP'12, Rostock, August 2012, WEP14.

[5] T. Galek et al., "Traveling Poles Elimination Scheme and Calculations of External Quality Factors of HOMs in SC Cavities", ICAP'12, Rostock, August 2012, WEP07.

[6] N. Valles and M. Liepe, "Seven-cell Cavity Optimization for Cornell's Energy Recovery Linac", SRF'09, Berlin, September 2009, THPPO008, p. 538.

[7] F. Marhauser, "JLab High Current Cryomodule Development", ERL'09, Ithaca NY, September 2009, WG307.

[8] A. Neumann et al., "Status of the HOM calculations for the BERLinPro main linac cavity", ICAP'12, Rostock, August 2012, FRAAC3.

[9] T. Flisgen et al., "Lumped equivalent models of complex RF structures", ICAP'12, Rostock, August 2012, THACI1.

[10] Computer Simulation Technology AG, Microwave Studio®, 64289 Darmstadt, Germany http://www.cst.com

[11] K. Rothemund, H.-W. Glock, U. van Rienen, "Eigenmode calculation of complex rf-structures using S-parameters", (2000) IEEE Transactions on Magnetics, 36 (4 I), pp. 1501-1503.